Greenhouse Effect in Semi-Infinite Scattering Atmospheres

R. E. Samuelson

Goddard Space Flight Center, Greenbelt, Maryland

ABSTRACT

The method of discrete ordinates is extended to describe the steady state intensity distribution of thermal radiation and the corresponding depth-dependent thermal structure of a plane-parallel semi-infinite particulate medium in radiative equilibrium in the presence of an outside point source of visible radiation. The greenhouse factor [$B(\tau) / F(0)$] is found to approach a finite limit as $\tau \rightarrow \infty$. Numerical calculations show that the diffuse field of visible radiation generated by multiple scattering processes is extremely effective in heating the lower regions of a particulate atmosphere. For slightly more realistic single scattering parameters than those considered in this study, it would appear that the large differences in temperature between the surface and the effective level of infrared radiation of Venus, as inferred from the infrared and microwave observations, can be mostly accounted for. Neither high surface pressures nor internal heat sources are required to make the heating mechanism work effectively.

I. INTRODUCTION

It has been demonstrated (King, 1963) that under certain conditions the temperature of a planetary atmosphere in radiative equilibrium increases with optical depth, even though the sole source of heating decreases exponentially with optical depth. The major requirement for a strong greenhouse effect appears to be that the ratio of the infrared to visible absorption coefficients be fairly large at most infrared wavelengths. Frequent and fairly wide infrared windows are the rule for atmospheres containing realistic amounts of optically active gases. In general such windows do not exist, however, for atmospheres composed of particles of a few microns in diameter. Exceptions to this rule are likely to occur in rather narrow spectral intervals just to the shorter wavelength side of regions of anomolous dispersion, where the real part of the refractive index of the relevant substance is close to unity. For this and several other reasons to be discussed it would seem germane to investigate the role that particulate matter plays in giving rise to strong greenhouse effects. In order to do this in any proper sense it is mandatory to include anisotropic scattering effects in solving the appropriate equation of radiative transfer.

II. SOLAR HEATING

Consider first the diffuse field of visible radiation arising from sunlight multiply scattered in a particulate atmosphere. Approximating the sun as a point source, the equation of transfer becomes (Chandrasekhar, 1960; henceforth referred to as R. T.)

$$\mu \frac{dI(\tau,\mu,\phi)}{d\tau} = I(\tau,\mu,\phi) - \frac{1}{4\pi}\int_0^{2\pi}\int_{-1}^{+1} p(\mu,\phi;\mu',\phi') I(\tau,\mu',\phi')\, d\mu' d\phi' - \frac{1}{4} F_0 e^{-\tau/\mu_0} p(\mu,\phi;-\mu_0,\phi_0) , \tag{1}$$

where the symbols have the same meaning as in R.T.. In particular, πF_0 is the flux of direct visible radiation from the sun which crosses a unit area normal to the beam.

It will be assumed throughout this study that the atmosphere in question is grey with respect to both visible and infrared radiation, although the two wavelength regions will be considered as having two different greyness parameters. By this is meant that the scattering and absorption properties of the atmosphere are the same throughout each of the two spectral regions, but that the atmospheric properties become different in going from one to the other. Thus (1) is independent of wavelength.

As is customary, we assume the intensity in (1) to be of the form

$$I(\tau,\mu,\phi) = \sum_{m=0}^{N} I^{(m)}(\tau,\mu)\cos m(\phi_0-\phi), \tag{2}$$

and the phase function for single scattering representable by the finite series expansion of Legendre polynomials:

$$p(\mu,\phi;\mu',\phi') = \sum_{\ell=0}^{N} \omega_\ell P_\ell(\cos\Theta), \tag{3}$$

where Θ is the angle through which radiation is singly scattered. As is demonstrated in R.T., equation (1) separates into (N + 1) linearly independent equations. In particular, the azimuth-independent term in (2) obeys the equation

$$\mu \frac{dI^{(0)}(\tau,\mu)}{d\tau} = I^{(0)}(\tau,\mu) - \frac{1}{2}\int_{-1}^{+1}\left[\sum_{\ell=0}^{N}\omega_\ell P_\ell(\mu)P_\ell(\mu')\right] I^{(0)}(\tau,\mu')\,d\mu' - \frac{1}{4}F_0 e^{-\tau/\mu_0}\sum_{\ell=0}^{N}\omega_\ell P_\ell(\mu)P_\ell(-\mu_0). \tag{4}$$

The solution to (4) by the method of discrete ordinates is

$$I^{(0)}(\tau,\mu_i) = \frac{1}{4}F_0\left\{\sum_{\alpha=1}^{n}\frac{L_\alpha e^{-k_\alpha\tau}}{1+\mu_i k_\alpha}\left[\sum_{\ell=0}^{N}\omega_\ell \xi_\ell(+k_\alpha)P_\ell(\mu_i)\right] + \frac{\gamma_0 e^{-\tau/\mu_0}}{1+\mu_i/\mu_0}\left[\sum_{\ell=0}^{N}\omega_\ell \xi_\ell\left(\frac{1}{\mu_0}\right)P_\ell(\mu_i)\right]\right\} \quad (i=\pm1,\ldots,\pm n), \tag{5}$$

where the cosine of the zenith angle μ is evaluated at the 2n discrete intervals $\pm\mu_i$ (i = 1, ..., n). As in R.T., the symbols γ_0 and ξ_ℓ are defined by the expressions:

$$\gamma_0 = H(\mu_0)\, H(-\mu_0) \tag{6}$$

where

$$H(x) = \frac{1}{\mu_1 \cdots \mu_n} \frac{\prod_{i=1}^{n} (x+\mu_i)}{\prod_{\alpha=1}^{n} (1+k_\alpha x)}\,, \tag{7}$$

and

$$\xi_\ell(x) = \sum_{\lambda=0}^{N} \omega_\lambda\, \xi_\lambda(x)\, D_{\ell,\lambda}(x) \qquad (\ell = 0, \ldots, N) \tag{8}$$

where

$$D_{\ell,\lambda}(x) = \frac{1}{2} \sum_{i} a_i \frac{P_\ell(\mu_i)\, P_\lambda(\mu_i)}{1+\mu_i x} \qquad (\lambda = \pm 1, \ldots, \pm n), \tag{9}$$

and where the a_i's are the usual Gaussian weights determined in accordance with the relation

$$a_i = \left(\frac{dP_{2n}(\mu)}{d\mu} \right)^{-1}_{\mu=\mu_i} \int_{-1}^{+1} \frac{P_{2n}(\mu)}{\mu - \mu_i}\, d\mu\,. \tag{10}$$

An alternative expression for ξ_ℓ is given by the recursion relation

$$\xi_{\ell+1}(\varkappa) = -\frac{2\ell+1-\varpi_\ell}{\varkappa(\ell+1)}\xi_\ell(\varkappa) - \frac{\ell}{\ell+1}\xi_{\ell-1}(\varkappa) . \tag{11}$$

In both (8) and (11)

$$\left.\begin{aligned} \xi_0(\varkappa) &= 1 \\ \xi_\lambda(\varkappa) &= 0 \quad (\lambda<0) \end{aligned}\right\} . \tag{12}$$

The n constants of integration L_α in (5) may be evaluated by imposing the n boundary conditions

$$I^{(0)}(0,-\mu_i) = 0 \qquad (i=1,\ldots,n) . \tag{13}$$

We shall be interested solely in the atmospheric heating caused by the incident solar radiation. For this purpose an expression is required for the flux divergence of the <u>total</u> visible radiation field. In this context the azimuth-dependent terms in (2) contribute nothing, and we shall neglect them.

The expression for the net flux $\pi F_T(\tau)$ of the <u>diffuse</u> radiation field, with the aid of (9) and the definition

$$\gamma_\ell = \gamma_0 \xi_\ell\left(\frac{1}{\mu_0}\right) , \tag{14}$$

becomes

$$F_T(\tau) = 2\sum_i a_i \mu_i I^{(\omega)}(\tau, \mu_i) \tag{15}$$

$$= F_0\left\{\sum_{\alpha=1}^{n} L_\alpha e^{-k_\alpha \tau}\left[\sum_{\ell=0}^{N} \tilde{\omega}_\ell \xi_\ell(+k_\alpha) D_{1,\ell}(+k_\alpha)\right] + e^{-\tau/\mu_0}\sum_{\ell=0}^{N} \tilde{\omega}_\ell \gamma_\ell D_{1,\ell}\left(\frac{1}{\mu_0}\right)\right\}.$$

By virtue of (8) and the relation* (R.T., page 154)

$$\gamma_\ell = P_\ell(-\mu_0) + \sum_{\lambda=0}^{N} \tilde{\omega}_\lambda \gamma_\lambda D_{\ell,\lambda}\left(\frac{1}{\mu_0}\right) \qquad (\ell = 0, \ldots, N), \tag{16}$$

equation (15) becomes

$$F_T(\tau) = F_0\left\{\sum_{\alpha=1}^{n} L_\alpha e^{-k_\alpha \tau} \xi_1(+k_\alpha) + \left[\gamma_1 + \mu_0\right] e^{-\tau/\mu_0}\right\}, \tag{17}$$

or, from (11), (12), and (14):

$$F_T(\tau) = F_0\left\{\mu_0 e^{-\tau/\mu_0} - (1-\tilde{\omega}_0^{\nu})\left[\sum_{\alpha=1}^{n} \frac{L_\alpha}{k_\alpha} e^{-k_\alpha \tau} + \mu_0 \gamma_0 e^{-\tau/\mu_0}\right]\right\}, \tag{18}$$

where $\tilde{\omega}_0^{\nu}$, the albedo for single scattering in the visible, is superscripted with a "V" to differentiate it from the albedo for single scattering in the infrared.

*The term $P_\ell(-\mu_0)$ in (16) was omitted in a previous report (Samuelson, 1965), and invalidates the subsequent derivation for $F_T(\tau)$. Equations C10 through C20 and also equation 96 of the report, which depend upon the derivation, are consequently incorrect.

The net flux $\pi F_0(\tau)$ of the attenuated direct radiation from the sun in the direction $-\mu_0$ and at a level τ is clearly given by

$$F_0(\tau) = -\mu_0 F_0 e^{-\tau/\mu_0} \tag{19}$$

The net flux $\pi F(\tau)$ of the total visible radiation field must be the sum of $\pi F_T(\tau)$ and $\pi F_0(\tau)$. Hence, from (18) and (19),

$$F(\tau_v) = -(1-\varpi_0^v) F_0 \left\{ \sum_{\alpha=1}^{n} \frac{L_\alpha}{k_\alpha} e^{-k_\alpha \tau_v} + \mu_0 \gamma_0 e^{-\tau_v/\mu_0} \right\}, \tag{20}$$

where τ_v is the optical depth in the visible. Differentiating (20) with respect to τ_v we obtain for the flux divergence (apart from the factor π):

$$\frac{dF(\tau_v)}{d\tau_v} = (1-\varpi_0^v) F_0 \left\{ \sum_{\alpha=1}^{n} L_\alpha e^{-k_\alpha \tau_v} + \gamma_0 e^{-\tau_v/\mu_0} \right\}. \tag{21}$$

III. RADIATIVE EQUILIBRIUM : THE TEMPERATURE PROFILE

We now assume (King, 1963) that the flux divergence in the visible must equal the flux divergence in the infrared; i.e., in a steady state there are no sources or sinks of radiation internal to the atmosphere. This is what shall be meant by an atmosphere in radiative equilibrium. For a quantitative comparison we shall need an expression analogous to (21) for the infrared.

The appropriate equation of transfer for a partially thermally emitting, partially anisotropically scattering semi-infinite atmosphere is (Samuelson, 1965; henceforth referred to as R-215)

$$\mu \frac{dI(\tau,\mu)}{d\tau} = I(\tau,\mu) - \frac{1}{2}\int_{-1}^{+1} p(\mu,\mu') I(\tau,\mu')\, d\mu' - (1-\varpi_0^\circ) B(\tau), \qquad (22)$$

where $B(\tau)$ is the Planck function in units of specific intensity and integrated over all (infrared) wavelengths, and

$$p(\mu,\mu') = \sum_{\ell=0}^{N} \varpi_\ell^\circ P_\ell(\mu) P_\ell(\mu'). \qquad (23)$$

All parameters in (22) refer now to the infrared, and are not to be confused with previous parameters referring only to the visible.

In particular $\tilde{\omega}_0^0$ is the albedo for single scattering in the infrared.

We may obtain an expression for $B(\tau)$ by multiplying through both sides of (22) by $d\mu$ and integrating over the interval $(-1 \leq \mu \leq +1)$. With the aid of (23), the identity

$$\int_{-1}^{+1} P_\ell(\mu) P_\lambda(\mu)\, d\mu = \begin{cases} 0 & (\ell \neq \lambda) \\ \frac{2}{2\ell+1} & (\ell = \lambda) \end{cases} , \tag{24}$$

and the definition for the flux integral,

$$F(\tau) = 2 \int_{-1}^{+1} \mu I(\tau, \mu)\, d\mu , \tag{25}$$

a straightforward evaluation yields

$$B(\tau) = \tfrac{1}{2} \int_{-1}^{+1} I(\tau, \mu)\, d\mu - \frac{1}{4(1-\tilde{\omega}_0^0)} \frac{dF(\tau)}{d\tau} , \tag{26}$$

and (22) becomes

$$\mu \frac{dI(\tau,\mu)}{d\tau} = I(\tau,\mu) - \tfrac{1}{2} \sum_{\ell=0}^{N} \tilde{\omega}_\ell P_\ell(\mu) \int_{-1}^{+1} P_\ell(\mu') I(\tau,\mu')\, d\mu' + \tfrac{1}{4} \frac{dF(\tau)}{d\tau} , \tag{27}$$

where

$$\left.\begin{aligned} \tilde{\omega}_\ell &= \tilde{\omega}_\ell^0 \quad (\ell = 1, \ldots, N) \\ \tilde{\omega}_0 &= 1 \end{aligned}\right\} . \tag{28}$$

This is to be compared with equation (3) in King's (1963) paper.

We now require in accordance with King that

$$\frac{dF(\tau_{IR})}{dz} = -\frac{dF(\tau_V)}{dz} \,, \tag{29}$$

where z is the vertical distance measured from some reference height (e.g. z_o) to the height of interest.

By definition

$$d\tau_V = -N_0(z)\,\chi_E^V\,dz \tag{30}$$

and

$$d\tau_{IR} = -N_0(z)\,\chi_E^{IR}\,dz \,, \tag{31}$$

where $N_0(z)$ is the number of particles per unit volume at a level z and χ_E^V and χ_E^{IR} are the effective extinction (absorption plus scattering) cross-sections per particle in the visible and infrared respectively. We shall assume that the particles are spherical and homogeneous, and that the definitions of χ_E^V and χ_E^{IR} in terms of the Mie parameters as given in R-215, section 3, are valid.

Let

$$\beta = \frac{\chi_E^V}{\chi_E^{IR}} \,. \tag{32}$$

Then, from (30) and (31),

$$d\tau_V = \beta\, d\tau_{IR} \,, \tag{33}$$

or, if β is assumed to be independent of z:

$$\tau_V = \beta \tau_{IR} \,. \tag{34}$$

This latter assumption is of doubtful validity for realistic atmospheres.

By virtue of (21) and (29) - (34), equation (27) becomes

$$\mu \frac{dI(\tau,\mu)}{d\tau} = I(\tau,\mu) - \frac{1}{2}\sum_{\ell=0}^{N} \omega_\ell P_\ell(\mu) \int_{-1}^{+1} P_\ell(\mu') I(\tau,\mu')\, d\mu' - \frac{1}{4}(1-\tilde{\omega}_0^V)\beta F_0 \left\{ \sum_{\alpha=1}^{n} L_\alpha e^{-k_\alpha \beta \tau} + \gamma_0 e^{-\beta\tau/\mu_0} \right\}, \tag{35}$$

where $\tau = \tau_{IR}$. Since $\tilde{\omega}_0 = 1$ the homogeneous part of (35) is formally equivalent to conservative scattering. Denoting the solution to the homogeneous part by the subscript G, we have, by the method of discrete ordinates in the n^{th} approximation* (R.T., page 154):

$$I_G(\tau,\mu_i) = \text{constant} + \times \left\{ \sum_{\rho=1}^{n-1} \frac{M_\rho e^{-k_\rho \tau}}{1+\mu_i k_\rho} \left[\sum_{\ell=0}^{N} \omega_\ell \xi_\ell(+k_\rho) P_\ell(\mu_i) \right] + \left[\left(1 - \tfrac{1}{3}\omega_1\right)\tau + \mu_i \right] M_0 + M_n \right\} \quad (i = \pm 1, \ldots, \pm n), \tag{36}$$

*There is no necessity for solving both (4) and (35) in the same degree of approximation. It is done here merely for the sake of simplicity.

where k_ρ ($\rho = 1, \ldots, n-1$) are the n-1 positive nonzero roots of the characteristic equation [cf. (8)-(12)]

$$1 = \frac{1}{2}\sum_{i} a_i \left[\frac{\sum_{\lambda=0}^{N} \omega_\lambda \xi_\lambda(k_\rho) P_\lambda(\mu_i)}{1 + \mu_i k_\rho}\right] \qquad (i = \pm 1, \ldots, \pm n). \tag{37}$$

That $k=0$ is also a root satisfying (37) is a characteristic common to all problems formally equivalent to conservative scattering.

It is clear that the (n+1) constants M_ρ ($\rho = 1, \ldots, n-1$), M_0, and M_n cannot all be determined from conditions (13). We shall find presently in obtaining the complete solution to (35) that an appeal to the flux integral resolves the difficulty.

Consider the equation [cf. eq. (35)]

$$\mu \frac{dI(\tau,\mu)}{d\tau} = I(\tau,\mu) - \frac{1}{2}\sum_{l=0}^{N} \omega_l P_l(\mu) \int_{-1}^{+1} P_l(\mu') I(\tau,\mu')\, d\mu' - \frac{1}{4} C_\rho e^{-\eta\tau} \tag{38}$$

where C_ρ and η are constants. Assume a solution for a particular integral of (38) of the form

$$I_\rho(\tau,\mu) = \frac{1}{4} C_\rho g(\mu) e^{-\eta\tau}, \tag{39}$$

where $g(\mu)$ is a function of μ yet to be determined. In the scheme of the n^{th} approximation, upon replacing μ by μ_i ($i = \pm 1, \ldots, \pm n$)

and substituting for $I(\tau,\mu_i)$ in (38) according to (39), we obtain:

$$(1+\eta\mu_i)\,g(\mu_i) = \frac{1}{2}\sum_{\ell=0}^{N}\omega_\ell P_\ell(\mu_i)\left[\sum_j a_j P_\ell(\mu_j)\,g(\mu_j)\right] + 1 \qquad (j=\pm 1,\ldots,\pm n). \tag{40}$$

Therefore $g(\mu_i)$ is of the form

$$g(\mu_i) = \frac{1}{1+\eta\mu_i}\left[1+\sum_{\ell=0}^{N}\omega_\ell\,\varepsilon_\ell(\eta)\,P_\ell(\mu_i)\right], \tag{41}$$

where the constants $\varepsilon_\ell(\eta)$ are given by

$$\varepsilon_\ell(\eta) = \frac{1}{2}\sum_j a_j P_\ell(\mu_j)\,g(\mu_j) \qquad (\ell=0,\ldots,N). \tag{42}$$

Substituting in (40) according to (41) we obtain

$$\sum_{\ell=0}^{N}\omega_\ell\,\varepsilon_\ell(\eta)\,P_\ell(\mu_i) = \frac{1}{2}\sum_{\ell=0}^{N}\omega_\ell P_\ell(\mu_i)\left\{\sum_j \frac{a_j P_\ell(\mu_j)}{1+\eta\mu_j}\left[1+\sum_{\lambda=0}^{N}\omega_\lambda\,\varepsilon_\lambda(\eta)\,P_\lambda(\mu_j)\right]\right\}. \tag{43}$$

Since (43) is valid for all μ_i we obtain, after some reduction,

$$\varepsilon_\ell(\eta) = D_{\ell,0}(\eta) + \sum_{\lambda=0}^{N}\omega_\lambda\,\varepsilon_\lambda(\eta)\,D_{\ell,\lambda}(\eta) \qquad (\ell=0,\ldots,N), \tag{44}$$

where

$$D_{\ell,\lambda}(\eta) = \frac{1}{2} \sum_j a_j \frac{P_\ell(\mu_j) P_\lambda(\mu_j)}{1+\mu_j \eta} \quad . \tag{45}$$

Equation (44) yields an NxN system of equations which may then be solved for the N values of ε_ℓ for the argument η.

We may also obtain from (45) a recursion relation satisfying the D's:

$$(2\ell+1) D_{\ell,\lambda}(\eta) = \delta_{\ell,\lambda} - \eta \left[(\ell+1) D_{\ell+1,\lambda}(\eta) + \ell D_{\ell-1,\lambda}(\eta) \right] , \tag{46}$$

where $\delta_{\ell,\lambda}$ is the Kronecker δ-function. Along lines analogous to R.T., pages 154-155, we may use (44) and (46) to obtain the recursion relation satisfied by the ε's:

$$\varepsilon_{\ell+1}(\eta) = -\frac{2\ell+1-\omega_\ell}{\eta(\ell+1)} \varepsilon_\ell(\eta) - \frac{\ell}{\ell+1} \varepsilon_{\ell-1}(\eta) + \frac{\delta_{\ell,0}}{\eta(\ell+1)} \quad . \tag{47}$$

In particular ($\omega_0 = 1$):

$$\varepsilon_1(\eta) = \frac{1}{\eta} \quad , \tag{48}$$

a relation we will find useful in resolving the value of M_0 in (36).

It is clear that (47) provides an alternative method of evaluating all ε_ℓ ($\ell = 0, \ldots, N$) once the value of ε_0 is known.

We try a relation of the form

$$\varepsilon_\ell(\eta) = \varepsilon_\ell(\eta)\,\xi_\ell(\eta) + f_\ell(\eta)\ , \tag{49}$$

where $f_\ell(\eta)$ is unspecified for the moment. Substituting (49) into (44) we obtain

$$\varepsilon_\ell(\eta) = D_{\ell,0}(\eta) + \varepsilon_0(\eta)\sum_{\lambda=0}^{N}\varpi_\lambda\,\xi_\lambda(\eta)D_{\ell,\lambda}(\eta) + \sum_{\lambda=0}^{N}\varpi_\lambda\,f_\lambda(\eta)D_{\ell,\lambda}(\eta)\ ; \tag{50}$$

hence, upon setting $\ell = 0$:

$$\varepsilon_0(\eta) = \frac{D_{0,0}(\eta) + \sum_{\lambda=0}^{N}\varpi_\lambda\,f_\lambda(\eta)D_{0,\lambda}(\eta)}{1 - \sum_{\lambda=0}^{N}\varpi_\lambda\,\xi_\lambda(\eta)D_{0,\lambda}(\eta)}\ . \tag{51}$$

Again, substituting (49) into (47) we obtain, with the aid of (11), the relation

$$f_{\ell+1}(\eta) = -\frac{2\ell+1-\varpi_\ell}{\eta(\ell+1)}f_\ell(\eta) - \frac{\ell}{\ell+1}f_{\ell-1}(\eta) + \frac{\delta_{0,\ell}}{\eta(\ell+1)}\ , \tag{52}$$

where, according to (12) and (49):

$$f_0(\eta) = 0\ , \tag{53}$$

making (52) determinate for all ℓ. It appears possible to express at least part of (51) in terms of Chandrasekhar's H-functions; however, in the interest of conserving space, we shall not pursue the matter here.

By virtue of (41) the particular integral (39) becomes

$$I_p(\tau,\mu_i) = \tfrac{1}{4} C_p e^{-\beta\tau} \frac{1}{1+\beta/\mu_i}\left[1 + \sum_{l=0}^{N} \omega_l \varepsilon_l(\beta) P_l(\mu_i)\right] \qquad (i = \pm 1, \ldots, \pm n). \tag{54}$$

By analogy with (38) and (54), the solution to (35) is [cf. also (36)]

$$\begin{aligned} I(\tau,\mu_i) = \tfrac{1}{4}(1-\omega_0^{\nu})\beta F_0 \Bigg\{ & \sum_{\rho=1}^{n-1} \frac{M_\rho e^{-k_\rho \tau}}{1+\mu_i k_\rho}\left[\sum_{l=0}^{N} \omega_l \xi_l(k_\rho) P_l(\mu_i)\right] \\ & + \left[\left(1-\tfrac{1}{3}\omega_1\right)\tau + \mu_i\right] M_0 + M_n \\ & + \sum_{\alpha=1}^{n} \frac{L_\alpha e^{-k_\alpha \beta\tau}}{1+\mu_i k_\alpha \beta}\left[1 + \sum_{l=0}^{N} \omega_l \varepsilon_l(k_\alpha \beta) P_l(\mu_i)\right] \\ & + \frac{\gamma_0 e^{-\beta\tau/\mu_0}}{1+\mu_i \beta/\mu_0}\left[1 + \sum_{l=0}^{N} \omega_l \varepsilon_l\left(\frac{\beta}{\mu_0}\right) P_l(\mu_i)\right]\Bigg\} \qquad (i = \pm 1, \ldots, \pm n). \end{aligned} \tag{55}$$

The value of M_0 in (36) may be resolved in the following way. Substituting (55) into the flux integral

$$F(\tau) = 2 \sum_{i} a_i \mu_i I(\tau,\mu_i) \qquad (i = \pm 1, \ldots, \pm n) \tag{56}$$

we obtain with the aid of (45) successively the relations

$$F(\tau) = (1-\tilde{\omega}_0^{\nu})\beta F_0 \Bigg\{ \sum_{\rho=1}^{n-1} M_\rho e^{-k_\rho \tau} \Big[\sum_{\ell=0}^{N} \tilde{\omega}_\ell \, \xi_\ell(k_\rho) \Big(\frac{1}{2} \sum_i a_i \frac{\mu_i P_\ell(\mu_i)}{1+\mu_i k_\rho} \Big) \Big]$$

$$+ \Big[(1-\tfrac{1}{3}\tilde{\omega}_1)\tau M_0 + M_n \Big] \Big(\frac{1}{2} \sum_i a_i \mu_i \Big) + M_0 \Big(\frac{1}{2} \sum_i a_i \mu_i^2 \Big)$$

$$+ \sum_{\alpha=1}^{n} L_\alpha e^{-k_\alpha \beta \tau} \Big[\frac{1}{2} \sum_i a_i \frac{\mu_i}{1+\mu_i k_\alpha \beta} + \sum_{\ell=0}^{N} \tilde{\omega}_\ell \xi_\ell(k_\alpha \beta) \Big(\frac{1}{2} \sum_i a_i \frac{\mu_i P_\ell(\mu_i)}{1+\mu_i k_\alpha \beta} \Big) \Big]$$

$$+ \gamma_0 e^{-\beta\tau/\mu_0} \Big[\frac{1}{2} \sum_i a_i \frac{\mu_i}{1+\mu_i \beta/\mu_0} + \sum_{\ell=0}^{N} \tilde{\omega}_\ell \, \xi_\ell\Big(\frac{\beta}{\mu_0}\Big) \Big(\frac{1}{2} \sum_i a_i \frac{\mu_i P_\ell(\mu_i)}{1+\mu_i \beta/\mu_0} \Big) \Big] \Bigg\}$$

$$= (1-\tilde{\omega}_0^{\nu})\beta F_0 \Bigg\{ \sum_{\rho=1}^{n-1} M_\rho e^{-k_\rho \tau} \Big[\sum_{\ell=0}^{N} \tilde{\omega}_\ell \, \xi_\ell(k_\rho) D_{1,\ell}(k_\rho) \Big] + \frac{1}{3} M_0$$

$$+ \sum_{\alpha=1}^{n} L_\alpha e^{-k_\alpha \beta \tau} \Big[D_{1,0}(k_\alpha \beta) + \sum_{\ell=0}^{N} \tilde{\omega}_\ell \, \xi_\ell(k_\alpha \beta) D_{1,\ell}(k_\alpha \beta) \Big]$$

$$+ \gamma_0 e^{-\beta\tau/\mu_0} \Big[D_{1,0}\Big(\frac{\beta}{\mu_0}\Big) + \sum_{\ell=0}^{N} \tilde{\omega}_\ell \, \xi_\ell\Big(\frac{\beta}{\mu_0}\Big) D_{1,\ell}\Big(\frac{\beta}{\mu_0}\Big) \Big] \Bigg\} \,, \qquad (57)$$

or, by virtue of (8) and (44):

$$F(\tau) = (1-\varpi_0^v)\beta F_0 \left\{ \sum_{\rho=1}^{n-1} M_\rho e^{-k_\rho \tau} \xi_1(k_\rho) + \frac{1}{3} M_0 \right.$$

$$\left. + \sum_{\alpha=1}^{n} L_\alpha e^{-k_\alpha \beta \tau} \varepsilon_1(k_\alpha \beta) + \gamma_0 e^{-\beta\tau/\mu_0} \varepsilon_1\left(\frac{\beta}{\mu_0}\right) \right\} . \qquad (58)$$

Again, by (11), (12), and (48), since $\varpi_0 = 1$,

$$F(\tau) = (1-\varpi_0^v) F_0 \left\{ \frac{1}{3}\beta M_0 + \sum_{\alpha=1}^{n} \frac{L_\alpha}{k_\alpha} e^{-k_\alpha \beta \tau} + \mu_0 \gamma_0 e^{-\beta\tau/\mu_0} \right\}, \qquad (59)$$

or, from (20) and (34),

$$F(\tau) + F(\tau_v) = \frac{1}{3}(1-\varpi_0^v)\beta F_0 M_0 . \qquad (60)$$

In a steady state

$$F_{IR}(0) + F_v(0) = 0 \ ; \qquad (61)$$

hence M_0 is zero for $\beta \neq 0$, and quite generally (60) becomes

$$F(\tau_{IR}) + F(\tau_v) = 0 \qquad (\beta \neq 0) . \qquad (62)$$

Re-writing (55) and (59) we have

$$I(\tau,\mu_i) = \tfrac{1}{4}(1-\tilde{\omega}_0^{\nu})\beta F_0\Big\{\sum_{\rho=1}^{n-1}\frac{M_\rho e^{-k_\rho\tau}}{1+\mu_i k_\rho}\Big[\sum_{l=0}^{N}\tilde{\omega}_l\,\xi_l(k_\rho)P_l(\mu_i)\Big] + M_n$$

$$+\sum_{\alpha=1}^{n}\frac{L_\alpha e^{-k_\alpha\beta\tau}}{1+\mu_i k_\alpha\beta}\Big[1+\sum_{l=0}^{N}\tilde{\omega}_l\,\varepsilon_l(k_\alpha\beta)P_l(\mu_i)\Big]$$

$$+\frac{\gamma_0 e^{-\beta\tau/\mu_0}}{1+\mu_i\beta/\mu_0}\Big[1+\sum_{l=0}^{N}\tilde{\omega}_l\,\varepsilon_l\Big(\frac{\beta}{\mu_0}\Big)P_l(\mu_i)\Big]\Big\} \qquad (i=\pm1,\ldots,\pm n) \tag{63}$$

and

$$F(\tau) = (1-\tilde{\omega}_0^{\nu})F_0\Big\{\sum_{\alpha=1}^{n}\frac{L_\alpha}{k_\alpha}e^{-k_\alpha\beta\tau} + \mu_0\gamma_0 e^{-\beta\tau/\mu_0}\Big\}, \tag{64}$$

from which it follows that [cf. also (21) and (29)-(34)]

$$\frac{dF(\tau)}{d\tau} = -(1-\tilde{\omega}_0^{\nu})\beta F_0\Big\{\sum_{\alpha=1}^{n}L_\alpha e^{-k_\alpha\beta\tau} + \gamma_0 e^{-\beta\tau/\mu_0}\Big\}. \tag{65}$$

In a fashion completely analogous to the derivation of (57) et seq. we may obtain the relations

$$\int_{-1}^{+1}I(\tau,\mu)\,d\mu \approx \sum_i a_i I(\tau,\mu_i) \qquad (i=\pm1,\ldots,\pm n)$$

$$= \tfrac{1}{2}(1-\tilde{\omega}_0^{\nu})\beta F_0\Big\{\sum_{\rho=1}^{n-1}M_\rho e^{-k_\rho\tau} + M_n$$

$$+\sum_{\alpha=1}^{n}L_\alpha\,\varepsilon_0(k_\alpha\beta)e^{-k_\alpha\beta\tau} + \gamma_0\,\varepsilon_0\Big(\frac{\beta}{\mu_0}\Big)e^{-\beta\tau/\mu_0}\Big\}. \tag{66}$$

Hence, from (65) and (66), expression (26) for the integrated Planck function becomes

$$B(\tau) = \frac{1}{4}(1-\bar{\omega}_0^{\nu})\beta F_0 \left\{ \sum_{\rho=1}^{n-1} M_\rho e^{-k_\rho \tau} + M_n \right.$$

$$\left. + \sum_{\alpha=1}^{n} L_\alpha \left[\frac{1}{1-\bar{\omega}_0^{\circ}} + \varepsilon_0(k_\alpha \beta) \right] e^{-k_\alpha \beta \tau} + \gamma_0 \left[\frac{1}{1-\bar{\omega}_0^{\circ}} + \varepsilon_0\left(\frac{\beta}{\mu_0}\right) \right] e^{-\beta\tau/\mu_0} \right\}. \quad (67)$$

The desired distribution of temperature with optical depth is given through the relation

$$B(\tau) = \frac{\sigma}{\pi} T^4(\tau) , \quad (68)$$

where $\sigma = 5.672 \times 10^{-12}$ watts/cm^2/deg^4.

It should be noted in (67) that $B(\tau)$ approaches a finite limit as $\tau \to \infty$. Hence, analogous to equation (25) of King's (1963) paper, we may define a greenhouse factor from (64) and (67) by the relation

$$B(\infty)/F(0) = \frac{1}{4}\beta M_n \left\{ \sum_{\alpha=1}^{n} \frac{L_\alpha}{k_\alpha} + \mu_0 \gamma_0 \right\}^{-1} . \quad (69)$$

The remainder of this study will be devoted to the numerical evaluation of some of the more relevant equations derived above for certain physically interesting situations. The results will be discussed in the context of the atmosphere of Venus.

IV. SINGLE SCATTERING

The atmosphere of Venus appears to support a cover of clouds sufficiently thick to obscure completely any trace of surface features. In addition this atmosphere may possibly support a large greenhouse effect (Sagan, 1962). It is of considerable practical importance, then, to investigate the role that clouds may play in the production of a greenhouse effect in the atmosphere of Venus. For the purpose of a preliminary reconnaissance of this general problem it would seem that a knowledge of the vertical temperature profiles and laws of darkening for a limited number of physically realistic model cloudy atmospheres, computed in accordance with the theory outlined above, would be of considerable interest. Before proceeding with such computations, however, it is necessary to adopt single scattering parameters appropriate to the atmosphere of Venus.

According to Sobolev (1963) the albedo for single scattering in the visible is very high ($\varpi_0^V = .989$). Although the high accuracy of the observational data from which Sobolev derived his value of ϖ_0^V has been only imperfectly demonstrated, it is felt that the superior quality of his work lends considerable weight to the essential correctness of the magnitude of this value. For the purpose of constructing a preliminary set of models the value $\varpi_0^V = .99$ has been adopted in this study.

In addition to the value of ϖ_o^V, it is necessary to assume values of several other parameters relevant for single scattering in both the visible and the infrared. To this end we shall assume that the particles of interest are spherical and homogeneous. For one such particle the size parameter α is given by

$$\alpha = \frac{2\pi r}{\lambda} , \tag{70}$$

where r is the particle radius and λ is the wavelength of radiation of interest. We shall adopt "effective" wavelengths of $\lambda_V = 5625$ Å and $\lambda_{IR} = 9\mu$ in the visible and infrared respectively, yielding an effective size parameter ratio for a single particle of

$$\alpha^V/\alpha^{IR} = 16 . \tag{71}$$

For the purpose of computational ease and uniqueness of solution it was decided to consider only square particle size distributions, i.e. distributions of particle sizes that are flat over the ranges of interest. Under the assumption of homogeneous spherical particles, the Mie theory was used to compute, for a variety of particle size distributions and complex indices of refraction, the following infrared single scattering parameters: (1) ϖ_o^o, the albedo for single scattering, (2) χ_ε^{IR}, the effective extinction cross-section per particle, and (3) $p(\cos\Theta)$, the phase function for single scattering. Eighteen values of the

complex index of refraction were used, covering the range ($1.1 - 0.01i \leq \tilde{n} \leq 1.6 - 0.50i$). In practice the particle size distributions considered were replaced by size parameter distributions over the range ($0 \leq \alpha \leq \alpha_0$). Sixteen values of α_0 were considered for each value of $\tilde{n}$.

The computed results indicated that $p(\cos\Theta)$ is very dependent upon α_0, but is almost independent of $\tilde{n}$. Hence, one mean phase function for each value of α_0 was considered sufficient to represent the angular distribution of singly scattered infrared radiation for a wide variety of possible substances, while three values of α_0 were chosen as being representative of a reasonable range of physically interesting conditions. These latter values, along with the corresponding values of β [cf. eq. (32)], $\tilde{\omega}_0^V$, $\tilde{\omega}_0^\circ$, and α_0^V are included in Table 1. The visible radiation single scattering parameters required to complete the table were calculated for an assumed index of refraction of $\tilde{n} = 1.33$; the imaginary part of $\tilde{n}$ was ignored, an approximation that should be acceptable in view of the high value of $\tilde{\omega}_0^V$. Values of $\alpha_0^{IR} < 1$ would tend to be physically uninteresting, because β would be quite large and the corresponding greenhouse effect quite small. On the other hand, values of $\alpha_0^{IR} > 4$ would not show much diversity since β would uniformly

remain about unity, and the single scattering patterns, both in the visible and the infrared, would change only slowly.

TABLE 1
Single Scattering Parameters

ϖ_o^V	ϖ_o^o	α_o^V	α_o^{IR}	$\beta = \frac{\chi_E^V}{\chi_E^{IR}}$
0.99	0.2	16	1	5
0.99	0.4	32	2	2
0.99	0.5	64	4	1

The relevant phase functions in the infrared, demonstrating the increase of the forward scattering lobe with increasing α_o^{IR}, are shown in Figure 1. Computations of $p(\cos\Theta)$ for the visible, however, cannot be disposed of so easily. It is possible to make the necessary computations for the values of α_o^V listed in Table 1, but the computer time required is rather excessive. However, the major difficulty stems from other considerations. The extreme nature of the forward scattering lobe of $p(\cos\Theta)$ for such large values of α_o^V requires a quite large value of N in a least-squares Legendre polynomial

fit of $p(\cos\Theta)$ in accordance with equation (3), and the computer program developed to solve the corresponding equation of transfer becomes unstable for values of N much in excess of N = 17. Refinements in the computational techniques become a matter of considerable delicacy beyond this point, and high values of $\tilde{\omega}_o^v$ tend to compound the difficulties.

Rather than attack the problem directly it was decided to attempt an alternative approach. First, phase functions ($\tilde{n} = 1.33$) were computed from the Mie theory for $\alpha_o^v = 1$, 2, and 4, and then fitted by equation (3) for N = 13. Next, the maximum value of α_o^v was sought for which equation (3) would satisfactorily fit the rigorously computed phase function. In this way it was found that $\alpha_o^v = 6$ would yield a phase function that could be approximated by (3) everywhere to within one percent of the true value, and much better over the forward scattering lobe; larger values of α_o^v were found to yield unsatisfactory results. Finally, the scattering pattern for very large spheres ($\alpha_o^v >> 1$) for a refractive index of 1.33 was adopted from Table 21 on page 232 of van de Hulst's (1957) book. This phase function was calculated by van de Hulst from geometrical optics, neglecting diffraction effects.

The five phase functions mentioned above have been reproduced in Figure 2. The solid curves were computed from the rigorous Mie theory, except for van de Hulst's large sphere ($\alpha_o^v = \infty$) model. The dashed curve approximating the last phase function was computed from (3) for N = 13; in all other cases the approximate and exact phase functions are indistinguishable in the figure. We shall see in the next section how these five phase functions are used to approximate realistic limb functions and temperature profiles for the atmospheric models of interest.

V. TEMPERATURE PROFILES AND THE LAW OF DARKENING

We shall be interested in solving equations (67)-(68) for the temperature profile and (63) for the law of darkening ($\tau = 0$) for each of the models listed in Table 1. (In order to obtain absolute temperature determinations in conformity with the solar flux at the distance of Venus, we have adopted a solar constant $\pi F_o = 0.26$ watts/cm2). In addition we will want to obtain solutions for each of these models for varying zenith angles of incident solar radiation; for this purpose the values $\mu_o = 1.0$, 0.4, and 0.16 have been chosen to be representative of the range of interest.

It has already been remarked that the actual computations must be restricted to $\alpha_0^V \leq 6$ ($\alpha_0^V = \infty$ excepted). In order to obtain approximately correct results for the models listed in Table 1, we have introduced the following artifice.

Consider first the model $\{\varpi_0^V = .99;\ \varpi_0^0 = .5;\ \alpha_0^{IR} = 4;\ \beta = 1;\ \mu_0 = 1.0\}$; for this model $\alpha_0^V = 64$. It is required now to compute the temperature profile from (67) and (68), using instead of $\alpha_0^V = 64$ the values $\alpha_0^V = 1$, 2, 4, and 6. In the upper part of Figure 3 the temperatures thus computed from equations (67)-(68) for infrared optical depths of $\tau = 0, .1, 1, 10,$ and ∞ are plotted as a function of $1/\alpha_0^V$. It is now assumed that the radiation diffracted around spheres very large compared with the wavelength (i.e. $\alpha_0^V = \infty$) is contained completely in the forward direction ($\Theta = 0$). Physically this is the same thing as saying that the diffracted radiation does not contribute to the diffuse radiation field. According to the Mie theory, which includes the effects of diffraction rigorously, the limiting value of χ_E^V as $\alpha_0^V \longrightarrow \infty$ is $\chi_E^V = 2\chi_G$, where χ_G is the geometrical cross-section. One half of this limiting value of χ_E^V is due to diffraction effects. It would appear to be a fairly good approximation in the case of large spheres to assume that none of the diffracted radiation is lost from the radiation field, since the corresponding cross-section

from geometrical optics is just χ_6. Hence, a reasonable approximation to impose on the model we are concerned with in the limiting case of $\alpha_0^\nu = \infty$ is to (1) retain the scattering pattern calculated by van de Hulst, (2) reduce β by a factor of two, and, in order to account for no losses of diffracted radiation, (3) reduce $(1 - \tilde{\omega}_0^\nu)$ by a factor of two. The resulting single scattering parameters become $\{\tilde{\omega}_0^\nu = .98;\ \tilde{\omega}_0^\circ = .5;\ \alpha_0^{IR} = 4;\ \beta = .5\}$.

The temperatures resulting from a solution for this model for the optical depths of interest are included along the ordinate corresponding to $1/\alpha_0^\nu = 0$ in the upper part of Figure 3. With the addition of these last points the curves connecting points of equal τ can be drawn quite smoothly. In addition, the general character of each curve tends to imply that valid temperature profiles for any value of $\alpha_0^\nu > 1$ can be successfully extracted from the figure. Of course, the only temperature profile thus inferred having any physical significance is the one ($\alpha_0^\nu = 64$) we are interested in, and is indicated by the arrows in the upper part of the figure.

The lower part of Figure 3 contains a similar family of interpolation curves for the model $\{\tilde{\omega}_0^\nu = .99;\ \tilde{\omega}_0^\circ = .2;\ \alpha_0^{IR} = 1;\ \beta = 5;\ \mu_0 = .16\}$. For this model the limiting case $\alpha_0^\nu = \infty$ was calculated using values of $\beta = 2.5$ and $\tilde{\omega}_0^\nu = .98$. The arrows in the lower part of

of the figure refer this time to the physically meaningful value $\alpha_o^v = 16$. Notice in particular the peculiar nature of the curve along $\tau = 0$ relative to other curves for different values of τ.

The temperature profiles in Figures 4 and 5 refer for the most part to the upper and lower families of curves in Figure 3 respectively. The five left-most solid curves in each of the figures are the temperature profiles computed for the five size parameters $\alpha_o^v = 1, 2, 4, 6,$ and ∞, while the dashed curves are the temperature profiles interpolated for each of the two physically meaningful values of α_o^v. It is interesting to note that a temperature minimum exists for the cases in Figure 5 somewhere in the range ($.12 \leq \tau \leq .19$). For large zenith angles of the sun it appears that, under the proper conditions, the extreme upper part of a particulate atmosphere is heated primarily by direct solar radiation, while further down the heating is caused primarily by the diffuse radiation field. It would seem that the temperature minimum occurs where the effects of the two mechanisms are of about equal magnitude. The high surface temperatures obtained for the sun at the local zenith (Figure 4) are about the same as those reported by Clark and Kuz'min (1965) for Venus, and hence are quite suggestive that particulate matter may be of some significance in the generation and maintenance of a greenhouse effect in the atmosphere of Venus.

In order to test whether an increase in the forward scatttering of visible radiation (resulting in a deeper penetration into the atmosphere) could produce a significant increase in the temperatures at large optical depths, the case of complete forward scattering was considered. Physically this would require that all the scattered radiation was scattered into the direction $\theta = 0$. This may be effected mathematically by replacing ϖ_0^{ν} with zero and reducing β, in accordance with the original value of ϖ_0^{ν}, by the factor $(1 - \varpi_0^{\nu})$. Further considerations reveal that the constants L_α ($\alpha = 1, \ldots, n$) in the relevant equations [cf. eqs. (63) and (67)] should be set equal to zero, and the constant γ_0 identified with unity. The right-most solid curves in Figures 4 and 5 illustrate the resulting temperature profiles for the respective cases in a rather dramatic fashion. Physically these cases refer to large spheres having a refractive index of unity in the visible (with a small absorption component). It would appear, therefore, that one method of enhancing the greenhouse effect is merely to require a small index of refraction in the visible. Of course the extreme case of complete forward scattering will result in a planetary albedo of zero; hence, as the index of refraction in the visible is steadily reduced, the corresponding value of ϖ_0^{ν} must be steadily increased in order to maintain a constant planetary albedo.

Through the method of interpolation described above, temperature profiles for each of the three models listed in Table 1 were computed for solar direction cosines of $\mu_0 = 1.0$, 0.4, and 0.16, and the results depicted in Figure 6. It is readily apparent that the temperature profile is relatively insensitive to the particle size down to an optical depth of $\tau \sim 6$ for the models adopted, but becomes quite sensitive for $\tau > 10$. Notice that as β decreases the effective heating at large τ increases, as one would expect intuitively. Far more important than β is the effect of μ_0. The increase of temperature at all optical depths with increasing μ_0 is due to the corresponding increase of incident solar flux and decrease of planetary albedo. This latter effect is enhanced by the forward scattering nature of the individual particles.

Table 2 below lists the planetary albedos A and effective temperatures T_E computed for each of the nine models presented in Figure 6 in accordance with the relations

$$A = 1 - \frac{F(0)}{\mu_0 F_0} \tag{72}$$

and

$$F(0) = \frac{\sigma}{\pi} T_E^4 , \tag{73}$$

where F(0) follows from the flux integral (56). The values of $I(0,-\mu_i)$ $(i = 1, \ldots, 7)$ in (56) are identically zero by virtue of the boundary conditions imposed at the top of the atmosphere, while the required values of $I(0,\mu_i)$ $(i = 1, \ldots, 7)$ were obtained by interpolation procedures entirely analogous to those used for obtaining the temperature profiles previously discussed [cf. Fig. 3]; instead of interpolating along curves of equal τ, interpolations were made along curves of equal μ_i. These latter interpolations were equally as satisfactory in appearance as the former. The results are illustrated in Figure 7 in units of temperature.

TABLE 2

Planetary Albedos and Effective Temperatures

α_0^{IR}	μ_0					
	1.0		0.4		0.16	
	A	$T_E(^\circ K)$	A	$T_E(^\circ K)$	A	$T_E(^\circ K)$
1	0.442	399.8	0.614	290.1	0.720	212.9
2	0.434	401.4	0.602	292.2	0.712	214.5
4	0.430	402.1	0.598	292.9	0.707	215.3

The albedos in Table 2 appear to be somewhat on the low side compared with the observed values for Venus (cf. Kozyrev, 1954), while effective temperatures listed in the table average out appreciably higher than those observed for Venus (cf. Murray, Wildey, and Westphal, 1963), and the variation of T_E with μ_0 is nothing like that observed. Again, the laws of darkening illustrated in Figure 7 average out to be somewhat more extreme than those observed by Murray, et al., while the variation of the laws with μ_0 do not agree with the observations at all. In view of the low rotation rate (Carpenter and Goldstein, 1963) and high effective nighttime temperatures observed for Venus it is highly likely that strong convection and advection are the dominant modes of heat transfer in the atmosphere of the planet. Such modes of heat transfer would be expected to decrease horizontal temperature gradients initiated through radiative processes quite markedly. However, it is possible that surface temperatures of 600°K – 700°K near the equator and 450°K at the poles exist (Clark and Kuz'min, 1965), implying that large horizontal temperature gradients near the surface may well be present. It appears very likely in any event that heat transfer mechanisms other than radiative play a large role in maintaining the actual temperature profiles existing in the atmosphere of Venus. Never-

theless, the probability of radiative processes being responsible in part for generating the gross features of the actual vertical temperature distribution of the atmosphere cannot be ignored.

VI. CONCLUDING REMARKS

It has been demonstrated that a thick cloud of particulate matter suspended in an atmosphere of optically inactive gases is capable of supporting a rather large greenhouse effect. In some regards this greenhouse mechanism is particularly promising in the case of Venus. One point that has not been emphasized is concerned with the small vertical distances required to attain large atmospheric optical thicknesses. As an example, let $r = 2 \times 10^{-4}$ cm $\chi_\varepsilon^{IR} = 2\pi r^2$, and the particle density $N_o = 100$ particles/cm^3. A simple calculation in accordance with the rough relation [cf. eq. (31)]

$$\tau = N_o \chi_\varepsilon^{IR} z_o \tag{74}$$

shows that the height of the atmosphere z_o corresponding to an optical thickness of $\tau = 100$ is about $z_o \sim 40$ km. Hence there is no need to ascribe the high surface pressures to the atmosphere of Venus that is required by a greenhouse model based solely on the infrared blanketing properties of carbon dioxide and water vapor (Jastrow and Rasool, 1963).

It should be noted that Sobolev's (1963) value of $\tilde{\omega}_o^v = .989$ was inferred from a much more isotropic phase function in the visible than would be expected to be relevant for the atmosphere of Venus. This is borne out in the somewhat low planetary albedos (computed for $\tilde{\omega}_o^v = .99$) listed in Table 2 of the present study. It is reasonable, therefore, to suspect that the value of $\tilde{\omega}_o^v$ for Venus is considerably higher. In addition, it is unreasonable to neglect gaseous absorption and emission in the infrared in view of the substantial amounts of carbon dioxide known to exist in the atmosphere of Venus. An inclusion of these effects can only serve to reduce the values of β used in the present study, since absorption in the visible should be relatively minor by contrast. A reduction in β, in turn, will serve to raise the surface temperature without affecting the effective temperature T_E [cf. eq. (64)]. On the other hand, increasing $\tilde{\omega}_o^v$ will serve to reduce T_E, although it is not so obvious how the surface temperature will be affected. In any event it would appear likely that certain more realistic combinations of $\tilde{\omega}_o^v$ and β than those considered in this study would maintain or increase the high surface temperature and at the same time reduce T_E, i.e. increase the planetary albedo.

A quantitative parametric study, more complete than the one presented here, as well as an extension of the general theory to

nongrey atmospheres, would be of considerable interest. In addition, any effort made to be definitive in describing the thermal structure of the atmosphere of Venus without including convection as an important mode of heat transfer is probably useless. We intend to return to these and related topics at a later time.

The unfailing willingness of Mr. J. D. Barksdale to perform the many tasks involved in writing the major computer program and providing the required computations is hereby gratefully acknowledged.

REFERENCES

Carpenter, R.L., and Goldstein, R. 1963, Science, 139, 910.

Chandrasekhar, S. 1960, Radiative Transfer (New York : Dover Publications, Inc.)

Clark, B.G., and Kuz'min, A.D., 1965, Ap. J., 142, 23.

Hulst, H.C. van de, 1957, Light Scattering by Small Particles (New York : John Wiley & Sons).

Jastrow, R., and Rasool, S.I. 1963, Space Research III, ed. W. Priester (Amsterdam : North-Holland Publishing Co.), p. 1036.

King, Jean I.F., 1963, Icarus, 2, 359.

Kozyrev, N.A., 1954, Publ. Crimean Astroph. Obs., 12, 177.

Murray, Bruce C., Wildey, Robert L., and Westphal, James A. 1963, J. Geophys. Res., 68, 4813.

Sagan, C. 1962, Icarus, 1, 151.

Samuelson, R. E., 1965, Radiative Transfer in a Cloudy Atmosphere (NASA Technical Report R-215).

Sobolev, V.V., 1963, A Treatise on Radiative Transfer (New York : D. Van Nostrand Co., Inc.).

FIGURE CAPTIONS

Figure 1 - Phase functions for single scattering in the infrared, computed for square size parameter distributions over the range ($0 \leq \alpha^{IR} \leq \alpha_0^{IR}$). The curves are averages of 28 phase functions computed for various complex indices of refraction covering the range ($1.1 - 0.01\,i \leq \tilde{n} \leq 1.6 - 0.50\,i$).

Figure 2 - Phase functions for single scattering in the visible, computed for square size parameter distributions over the range ($0 \leq \alpha^{V} \leq \alpha_0^{V}$). The solid curves are the exact Mie calculations for a real index of refraction of $\tilde{n} = 1.33$, except for the case of $\alpha_0^V = \infty$ which was computed from geometrical optics (neglecting diffraction). The dashed curve is a 14-term Legendre polynomial approximation for the last case.

Figure 3 - Curves of temperature vs. optical depth used to interpolate for two T-τ relations for realistic size parameter maxima α_0^V. The arrows for the upper family of curves locate the relevant size parameter $\alpha_0^V = 64$, while the arrows for the lower set locate the value $\alpha_0^V = 16$.

Figure 4 - Temperature profiles for the model { $\tilde{\omega}_0^V = .99$; $\tilde{\omega}_0^{IR} = .5$; $\alpha_0^{IR} = 4$; $\beta = 1$; $\mu_0 = 1.0$ }. The temperature profile corresponding to the physically significant size parameter maximum $\alpha_0^V = 64$ as interpolated from Figure 3 is shown by the dashed curve. The right-most solid curve is the temperature profile computed for the limiting case of complete forward scattering from very large spheres.

Figure 5 - Temperature profiles for the model { $\varpi_0^V = .99$; $\varpi_0^o = .2$; $\alpha_0^{IR} = 1$; $\beta = 5$; $\mu_0 = .16$ }. The temperature profile corresponding to the physically significant size parameter maximum $\alpha_0^V = 16$ as interpolated from Figure 3 is shown by the dashed curve. The right-most solid curve is the temperature profile computed for the limiting case of complete forward scattering from very large spheres. Notice the transition from a linear to a logarithmic scale at $\tau = 1$.

Figure 6 - Temperature profiles for the models listed in Table 1 as interpolated in accordance with the discussion given in the text (cf. also Figure 3).

Figure 7 - The laws of darkening for the models listed in Table 1 as interpolated in accordance with the discussion given in the text. The corresponding temperature profiles are shown in Figure 6.

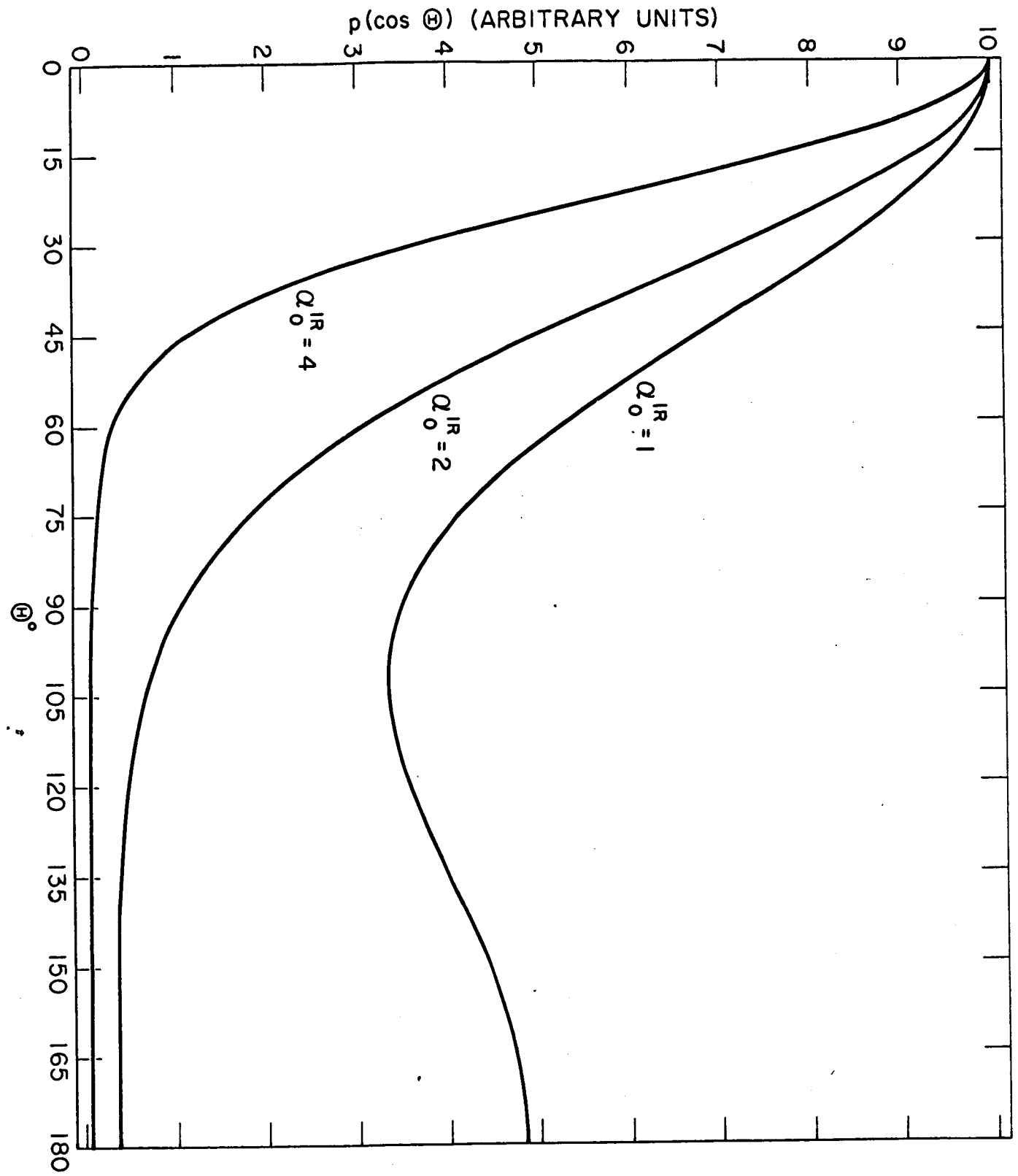
p(cos Θ) (ARBITRARY UNITS)
0
1
2
3
4
5
6
7
8
9
10
Θ°
0
15
30
45
60
75
90
105
120
135
150
165
180
$Q_o^{IR} = 4$
$Q_o^{IR} = 2$
$Q_o^{IR} = 1$

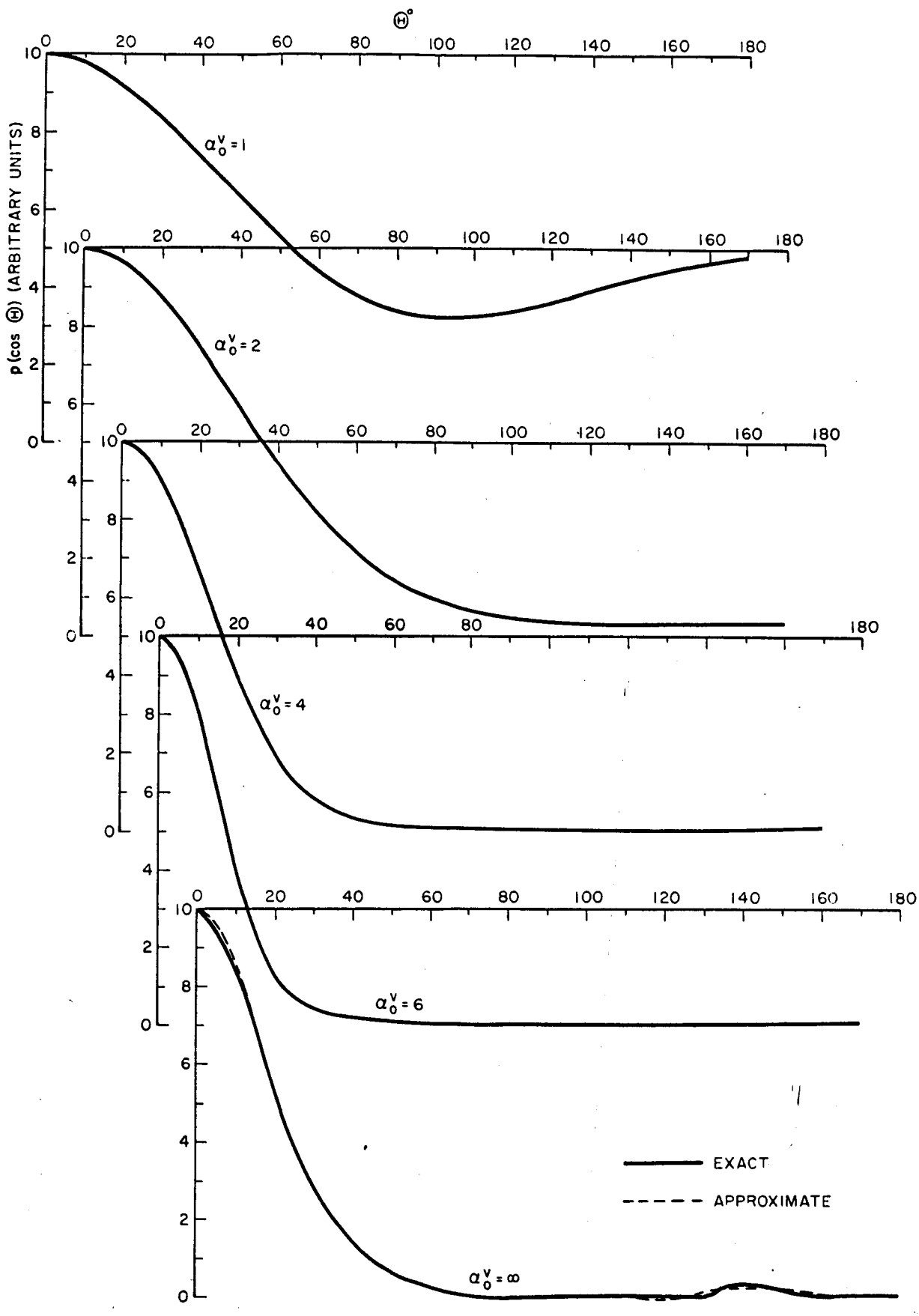
Θ°
0 20 40 60 80 100 120 140 160 180
p(cos Θ) (ARBITRARY UNITS)
0 2 4 6 8 10
$\alpha_0^v = 1$
$\alpha_0^v = 2$
$\alpha_0^v = 4$
$\alpha_0^v = 6$
$\alpha_0^v = \infty$
EXACT
APPROXIMATE

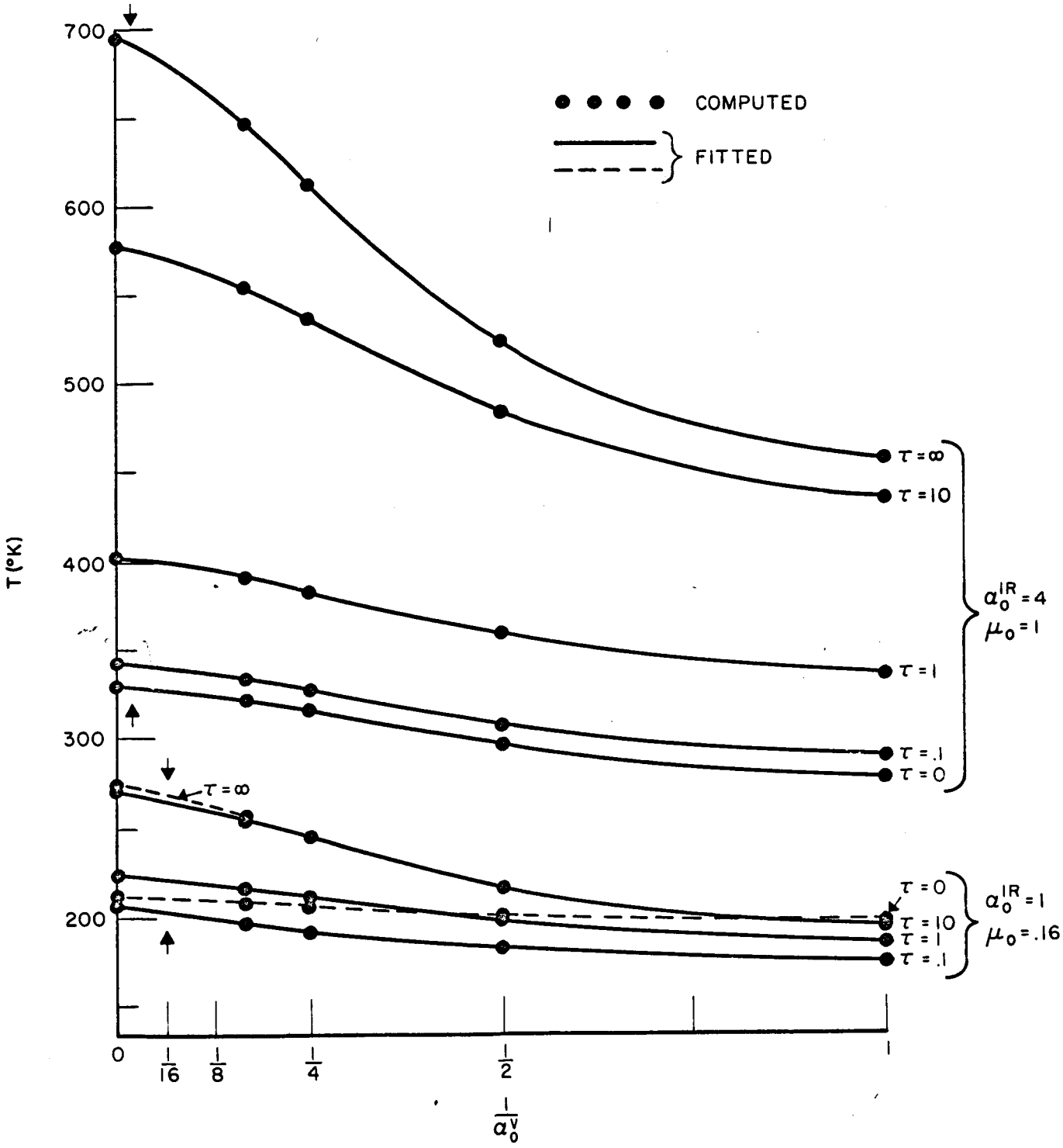
700
600
500
400
300
200
T (°K)
COMPUTED
FITTED
τ = ∞
τ = 10
τ = 1
τ = .1
τ = 0
$\alpha_0^{IR} = 4$
$\mu_0 = 1$
τ = ∞
τ = 0
τ = 10
τ = 1
τ = .1
$\alpha_0^{IR} = 1$
$\mu_0 = .16$
0
1/16
1/8
1/4
1/2
1
$\frac{1}{\alpha_0^V}$

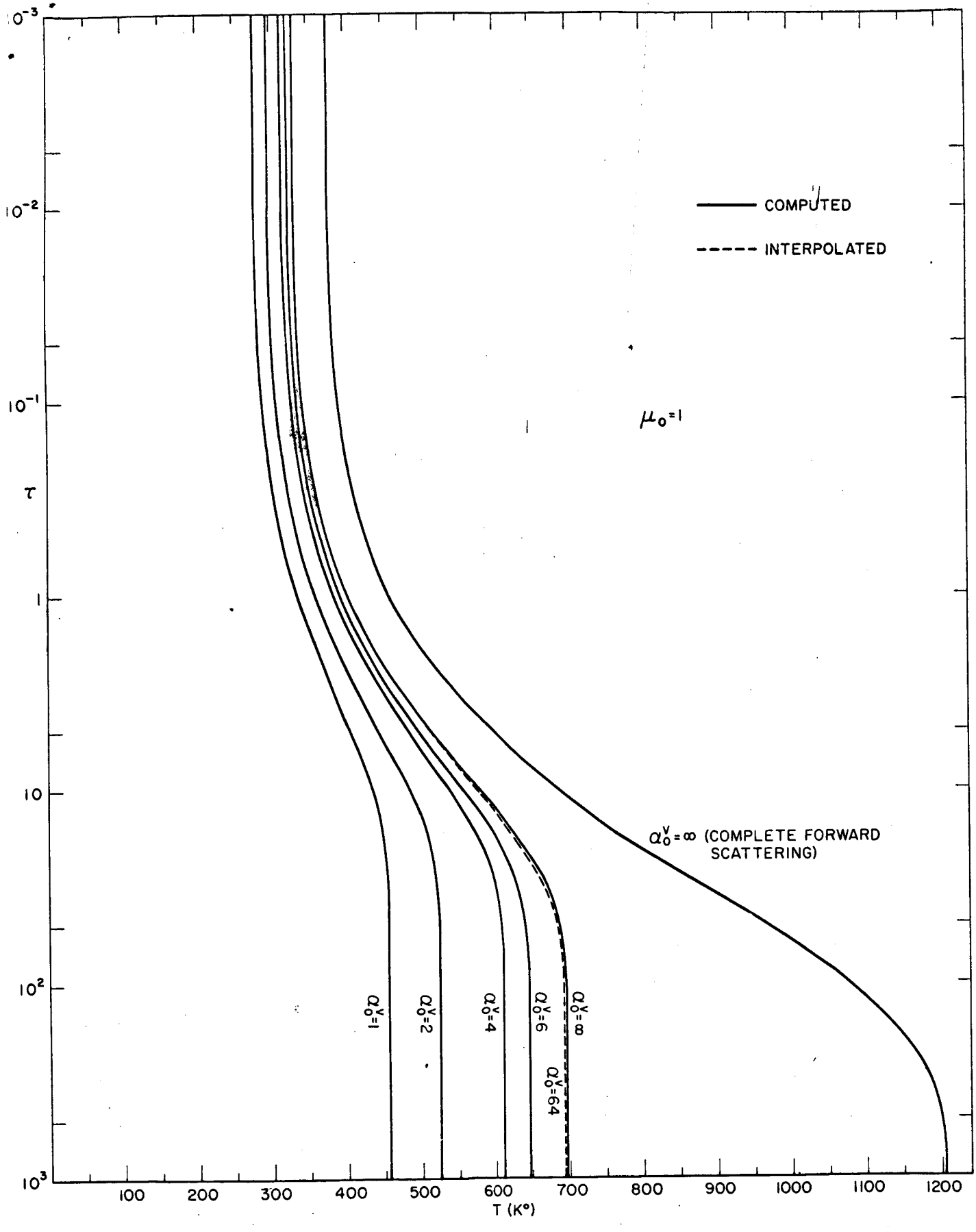
COMPUTED
INTERPOLATED
$\mu_0=1$
τ
10^{-3}
10^{-2}
10^{-1}
1
10
10^2
10^3
100
200
300
400
500
600
700
800
900
1000
1100
1200
T (K°)
$\alpha_0^v=\infty$ (COMPLETE FORWARD SCATTERING)
$\alpha_0^v=1$
$\alpha_0^v=2$
$\alpha_0^v=4$
$\alpha_0^v=6$
$\alpha_0^v=8$
$\alpha_0^v=64$

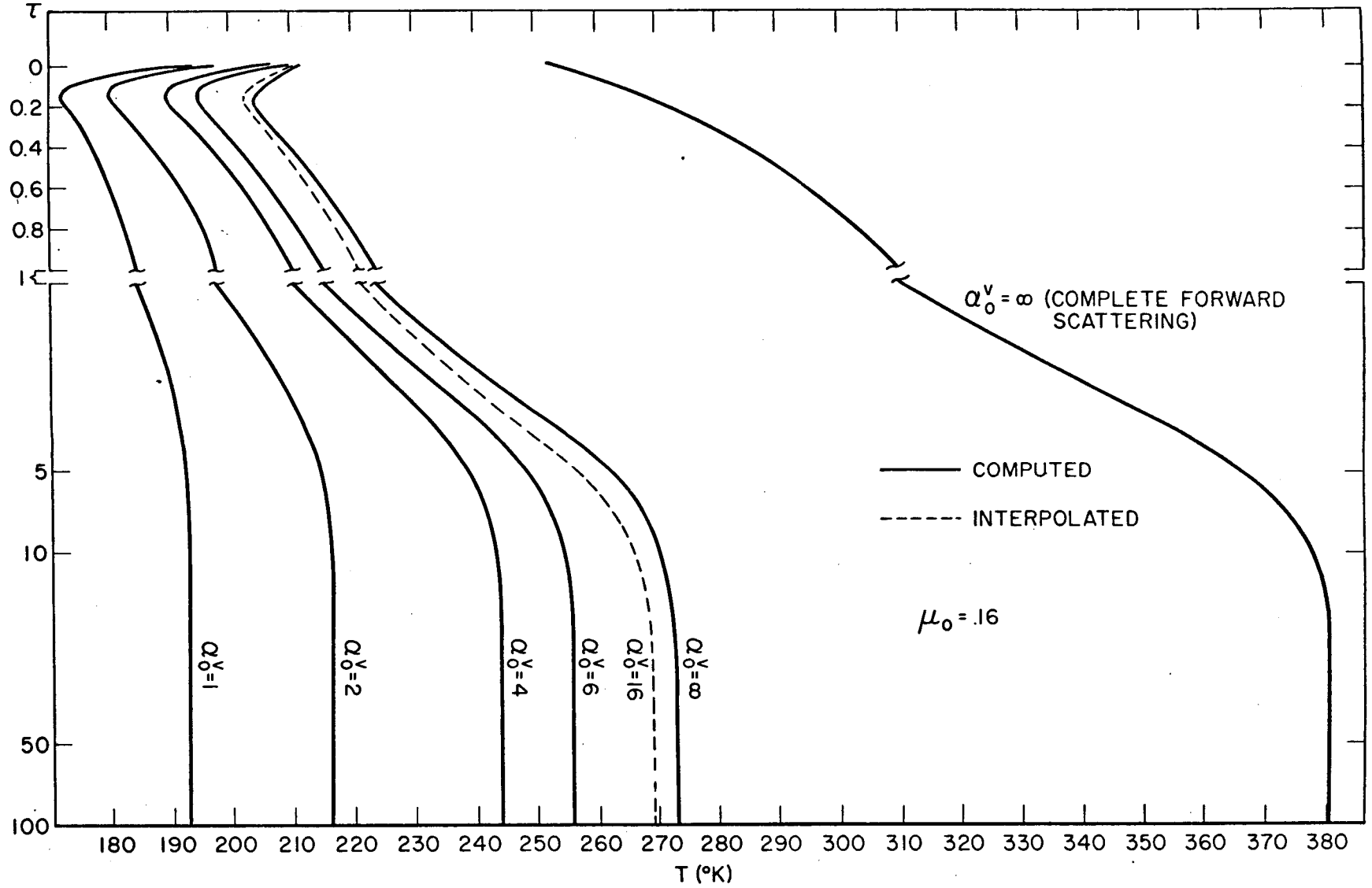
τ
0
0.2
0.4
0.6
0.8
1
5
10
50
100
180 190 200 210 220 230 240 250 260 270 280 290 300 310 320 330 340 350 360 370 380
T (°K)
$\alpha_0^v = \infty$ (COMPLETE FORWARD SCATTERING)
COMPUTED
INTERPOLATED
$\mu_0 = .16$
$\alpha_0^v = 1$
$\alpha_0^v = 2$
$\alpha_0^v = 4$
$\alpha_0^v = 6$
$\alpha_0^v = 16$
$\alpha_0^v = 8$

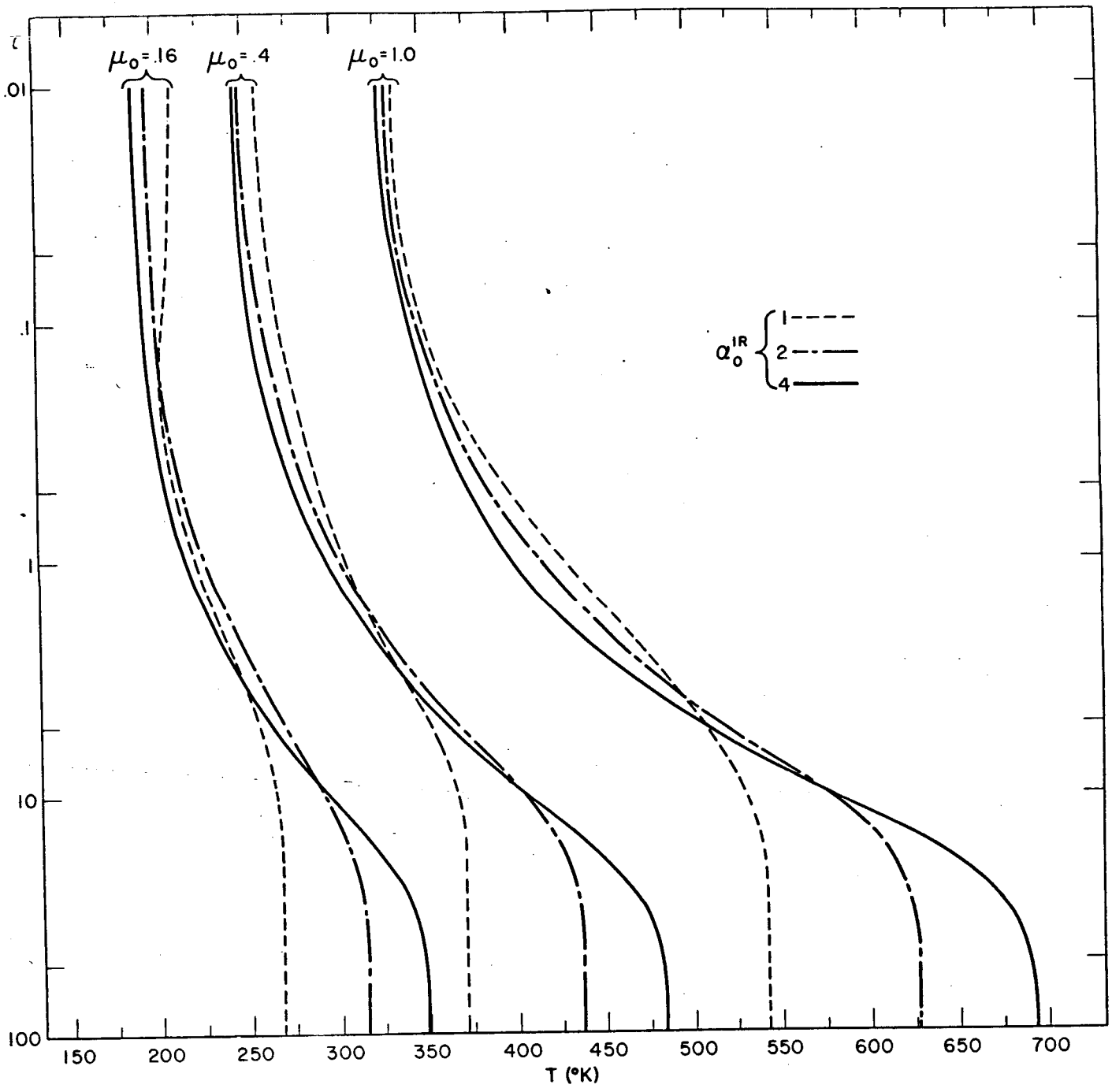
τ
.01
.1
1
10
100
μ_0=.16
μ_0=.4
μ_0=1.0
α_0^{IR}
1
2
4
150
200
250
300
350
400
450
500
550
600
650
700
T (°K)

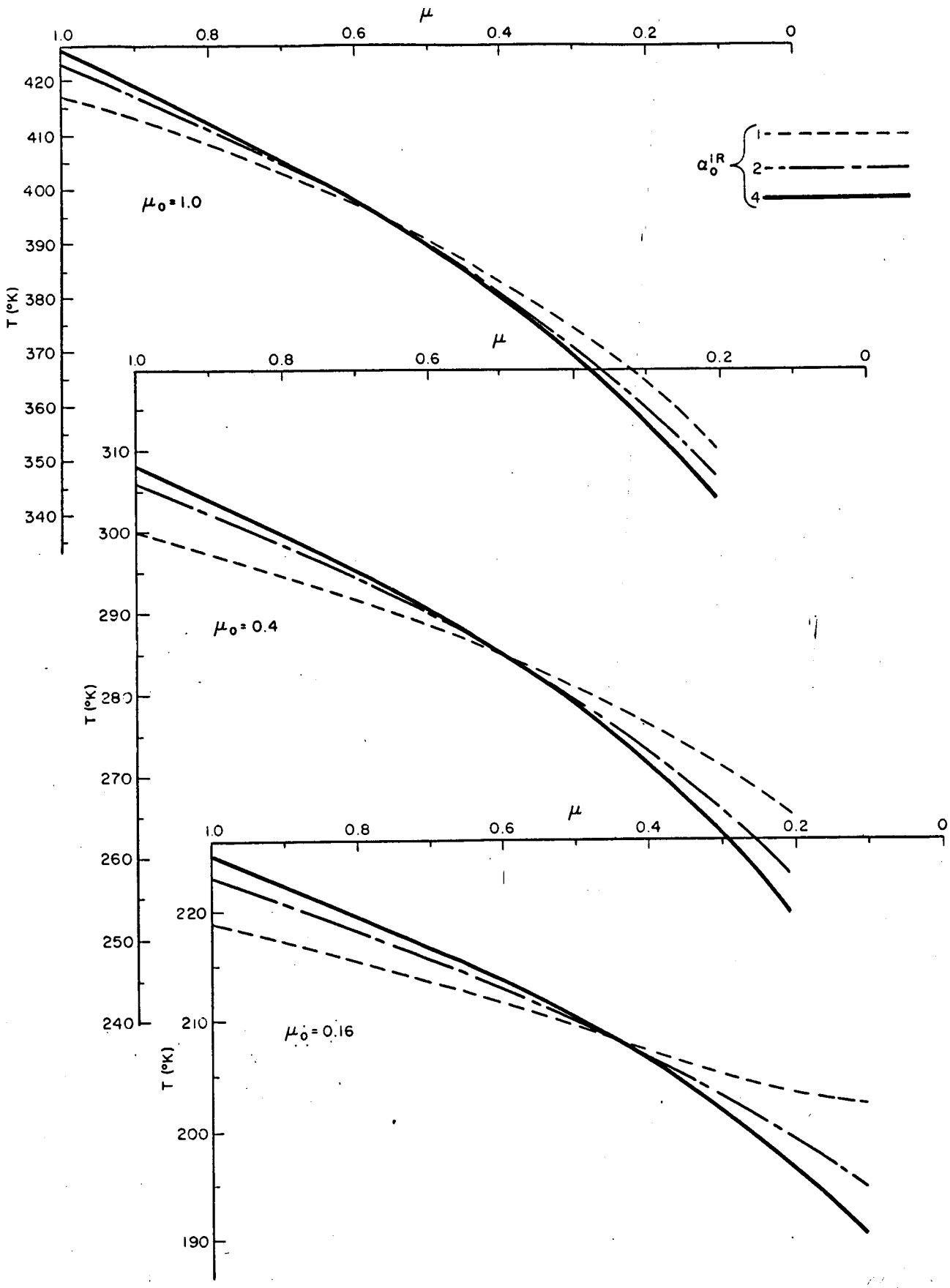
μ
1.0
0.8
0.6
0.4
0.2
0
T (°K)
420
410
400
390
380
370
360
350
340
$\mu_0 = 1.0$
α_0^{IR}
1
2
4
310
300
290
280
270
260
250
240
$\mu_0 = 0.4$
220
210
200
190
$\mu_0 = 0.16$